

Virtual rutting test of asphalt mixture using discrete element method

Zhang Deyu Huang Xiaoming Gao Ying

(School of Transportation, Southeast University, Nanjing 210096, China)

Abstract: In order to investigate the permanent deformation behavior of asphalt mixtures from discontinuity, the virtual rutting test of asphalt mixtures is developed by the discrete element method (DEM). A digital specimen generation procedure considering aggregate gradation and irregular shape is developed based on the probability theory and the Monte Carlo method. The virtual rutting test is then conducted based on the generated digital specimen. In addition, on the basis of the time-temperature superposition (TTS) principle, a calculation method is used to reduce the computation time of the virtual rutting test. The simulation results are compared with the laboratory measurements. The results show that the calculation method based on the TTS principle in the discrete element (DE) viscoelastic model can significantly reduce the computation time. The deformation law of asphalt mixtures in the virtual rutting test is similar to the laboratory measurements, and the deformation and the dynamic stability of the virtual rutting test are slightly greater than the laboratory measurements. The two-dimensional virtual rutting test can predict the permanent deformation performance of asphalt mixtures.

Key words: asphalt mixture; permanent deformation; discrete element method; virtual rutting test

doi: 10.3969/j.issn.1003-7985.2012.02.015

Rutting has become one of the major distresses in asphalt pavements, and it seriously affects driving safety and comfort. Many researchers have proposed research methods to investigate the permanent deformation behavior of asphalt mixtures, in which the traditional physical experiments are commonly used. However, the traditional methods are very time-consuming and costly, and the repeatability and reproducibility are poor^[1-2]. Therefore, many scholars have developed numerical modeling to investigate asphalt mixtures. The finite element method (FEM) and the boundary element method (BEM) have been widely used in numerical modeling. However, these methods are based on the assumption of

continuity, and there are some limitations in describing the discontinuity, heterogeneity and large strain of asphalt mixtures.

In recent years, the DEM has been gradually introduced into asphalt mixture studies. The DEM is suitable for analyzing discontinuous media, such as asphalt mixtures. It is based on successively solving Newton's second law for each particle and the force-displacement law for every contact. Chang and Meegoda^[3] proposed an innovative DEM model by modifying the TRUBAL program to describe different types of aggregate-aggregate and asphalt-aggregate contacts. You and Buttlar^[4-5] presented a 2D microfabric distinct element method (MDEM) to model the asphalt mixture microstructure and further predicted the dynamic modulus of asphalt mixtures across a range of temperatures and loading frequencies. Collop et al.^[6] investigated the use of distinct element modeling to simulate the behavior of a highly idealized bituminous mixture in uniaxial compressive creep tests. Abbas et al.^[7] presented a methodology for analyzing the viscoelastic response of asphalt mixtures using the DEM. The DEM models were subjected to sinusoidal loads similar to those applied in the simple performance test (SPT). The DEM model predictions compared favorably with the SPT measurements. Kim et al.^[8] applied the clustered DEM approach into the investigation of fracture mechanisms in asphalt concrete at low temperatures. A bilinear cohesive softening model was implemented into the DEM framework to enable the simulation of crack initiation and propagation in asphalt concrete.

By summarizing a number of the literature cited above, it is found that DE simulations mainly focus on stiffness prediction, fatigue modeling and fracture modeling, and few researches on permanent deformation behavior of asphalt mixtures using DEM have been conducted. Therefore, the 2D digital asphalt mixture specimen composed of coarse aggregates and asphalt mastic is generated in this paper. The virtual rutting test using the DEM is then developed and verified by laboratory measurements based on the generated digital specimen.

1 Generation of 2D Digital Specimen

1.1 2D quantity gradation of aggregate

Assuming that the aggregate is spherical, the probability that a circular plane with a diameter of d_j cuts from a

Received 2011-11-23.

Biographies: Zhang Deyu (1986—), male, graduate; Huang Xiaoming (corresponding author), male, doctor, professor, huangxm@seu.edu.cn.

Foundation item: The National Natural Science Foundation of China (No. 51108081).

Citation: Zhang Deyu, Huang Xiaoming, Gao Ying. Virtual rutting test of asphalt mixture using discrete element method[J]. Journal of Southeast University (English Edition), 2012, 28(2): 215 – 220. [doi: 10.3969/j.issn.1003-7985.2012.02.015]

sphere with a diameter of d_i is

$$P(D_c = d_j | D_s = d_i) \quad (1)$$

where D_c , D_s are the diameters of the circular plane and the spherical aggregate, respectively.

Assume that $P(D_c = d_j)$ is the probability that the circular planes with a diameter of d_j appear in the cross section of asphalt mixtures. $P(D_c = d_j)$ can be expressed as

$$P(D_c = d_j) = \sum P(D_s = d_i)P(D_c = d_j | D_s = d_i) \quad (2)$$

where $P(D_s = d_i)$ is the volume fraction of the aggregates with a diameter of d_j . Assuming that the aggregate densities are the same, the volume fraction can be derived by aggregate gradation.

According to Refs. [9–10], if the circular planes on the cross section are divided into m groups by diameter, the frequency of the aggregates with diameters ranging from d_j to d_{j+1} in group j is $N(D_c = d_j)$. If the aggregates are divided into n groups by diameter, the frequency of the aggregates with diameters ranging from d_i to d_{i+1} in group i is $N(D_s = d_i)$. The relationship between the two frequencies is

$$N(D_c = d_j) = 2\Delta \sum_{i=j}^n k_{ji} N(D_s = d_i) \quad (3)$$

$$k_{ji} = \begin{cases} 0 & j \neq i, j > i \\ \left[\left(i - \frac{1}{2} \right)^2 - (j-1)^2 \right]^{1/2} = \left(i - \frac{3}{4} \right)^{1/2} & i = j \\ \left[\left(i - \frac{1}{2} \right)^2 - (j-1)^2 \right]^{1/2} - \left[\left(i - \frac{1}{2} \right)^2 - j^2 \right]^{1/2} & j \neq i, j < i \end{cases} \quad (4)$$

where Δ is the diameter ranges of aggregate groups; k_{ji} is the contribution of the aggregate group with diameters ranging from d_i to d_{i+1} to the circular planes with diameters ranging from d_j to d_{j+1} in the cross section.

According to Eqs. (3) and (4), $M(D_c = d_j)$. The number of the circular planes with diameters ranging from d_j to d_{j+1} in the cross section of asphalt mixtures can be expressed as

$$M(D_c = d_j) = 2\Delta \sum_{i=j}^n k_{ji} M(D_s = d_i) \quad (5)$$

$$M(D_s = d_i) = \frac{48}{\pi(d_i + d_{i+1})^3} P(D_s = d_i) \quad (6)$$

where $M(D_s = d_i)$ is the number of the circular planes with diameters ranging from d_j to d_{j+1} .

Thus, the quantity gradation of 2D asphalt mixtures can be obtained according to Eqs. (4), (5) and (6). The mass gradation and the 2D quantity gradation of an asphalt mixture are listed in Tab. 1.

Tab. 1 Mass gradation and 2D quantity gradation of an asphalt mixture

Sieve size/ mm	Mass percentage passing/%	Quantity percentage passing/%
19.00	100	100
16.00	95	98
13.20	84	95
9.50	70	190
4.75	48	70
2.36	34	0

1.2 Generation of digital specimen

After quantity gradation is obtained, the 2D digital specimen of asphalt mixtures considering the irregular shape of aggregates is generated. It can be found that the aggregates on any cross section are polygons of edge numbers in the range [4, 10] when analyzing the aggregate shape by digital image processing. Therefore, aggregates are regarded as polygons with n edges, as shown in Fig. 1. The irregular shapes of aggregates in polar coordinates are controlled by

$$r_i = R_0 + (2\lambda - 1)R \quad (7)$$

$$\theta_i = \frac{2\pi[1 + (2\eta - 1)\delta]}{n} \quad (8)$$

where λ , η are the random numbers drawn from a uniform distribution in the range [0, 1]; R_0 is the average radius of aggregates; R is the size fluctuation; and δ is the number not greater than 1, indicating the angle fluctuation range. The irregular shapes of aggregates are controlled by both the aggregate radius fluctuation [$R_0 - R$, $R_0 + R$] and the angle fluctuation [$2\pi(1 - \delta)/n$, $2\pi(1 + \delta)/n$].

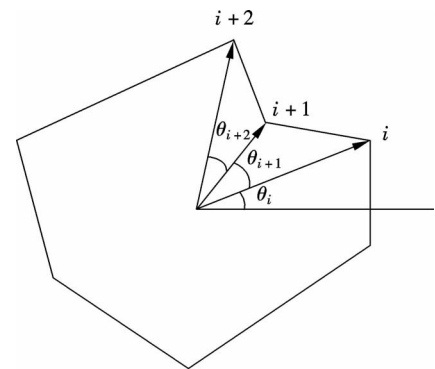


Fig. 1 Generation of aggregate with irregular shape

The generation program is developed by Microsoft Visual C++ 6.0 to achieve the visualization of the 2D digital specimen of asphalt mixtures based on the Monte Carlo method. The coarse aggregates (size ≥ 2.36 mm) with irregular shapes are randomly placed within the cross section of the specimen in accordance with the 2D quantity gradation as shown in Tab. 1. Coarse aggregates and asphalt mastic (fine aggregates, fines, and asphalt binder) constitute the 2D digital specimen as shown in Fig. 2.



Fig. 2 2D digital specimen of asphalt mixture

2 Virtual Rutting Test of Asphalt Mixture

2.1 Discrete element model of virtual specimen

The shape data of asphalt mixtures composed of 0 and 1 are obtained by Matlab and they are then imported into PFC2D, as shown in Fig. 3(a). Since air voids have a great impact on the permanent deformation behavior of asphalt mixtures, the air voids are introduced by randomly deleting a number of asphalt mastic elements. In this paper, the air void level is set to 4% as shown in Fig. 3(b). Thus, the virtual specimen with air voids is developed as shown in Fig. 3(c).

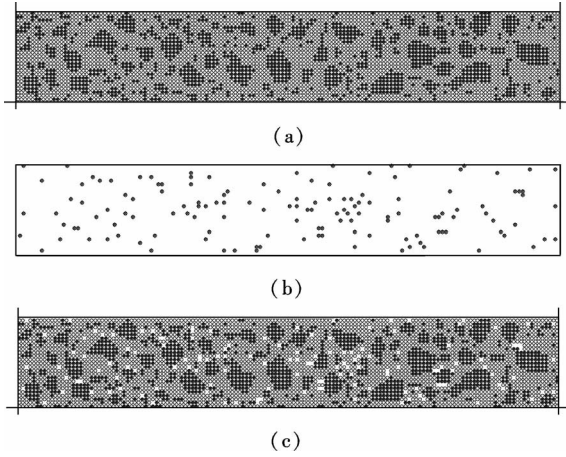


Fig. 3 DE model of virtual specimen. (a) DE model of virtual specimen without air voids; (b) Air voids distribution of virtual specimen; (c) DE model of virtual specimen with air voids

2.2 Micromechanical model and parameters

In the DE model of asphalt mixtures, there are four types of contacts to represent four different interactions: contacts within the asphalt mastic, contacts between the asphalt mastic and aggregates, contacts between adjacent aggregates, and contacts within aggregates.

Considering the viscoelastic behavior of the asphalt mastic, the Burger model (see Fig. 4) and the contact-bond model are employed to represent the interactions within the asphalt mastic and the interaction between the asphalt mastic and aggregates. The macroscale parameters of Burger's model used in this paper are fitted from the dynamic shear test as listed in Tab. 2. The conversion between microscale parameters of Burger's model (see Fig. 4) and the macroscale material properties are developed by Liu et al.^[11] as follows:

$$K_{mn} = E_1 t, \quad C_{mn} = \eta_1 t, \quad K_{kn} = E_2 t, \quad C_{kn} = \eta_2 t$$

$$K_{ms} = \frac{E_1 t}{2(1+\nu)}, \quad C_{ms} = \frac{\eta_1 t}{2(1+\nu)}$$

$$K_{ks} = \frac{E_2 t}{2(1+\nu)}, \quad C_{ks} = \frac{\eta_2 t}{2(1+\nu)}$$

where E_1 , η_1 , E_2 and η_2 are the macroscale parameters of Burger's model; K_{mn} , C_{mn} , K_{kn} and C_{kn} are the microscale parameters of Burger's model in the normal direction; K_{ms} , C_{ms} , K_{ks} and C_{ks} are the microscale parameters of Burger's model in the shear direction; t is the disk thickness; and ν is the Poisson ratio.

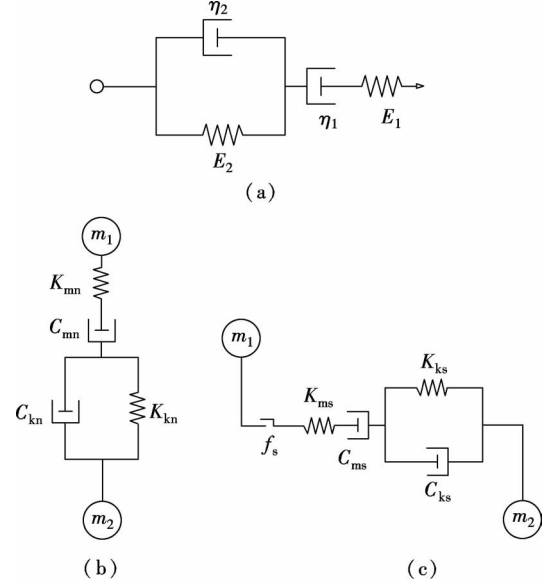


Fig. 4 Burger's model. (a) Macro behaviors; (b) Micro behaviors in the normal direction; (c) Micro behaviors in the shear direction

Tab. 2 Macroscale parameters of Burger's model at 60 °C

E_1 /MPa	η_1 /(MPa · s)	E_2 /MPa	η_2 /(MPa · s)
4.64	83.34	0.82	10.00

In this study, the aggregate is considered as a pure elastic material. The linear contact-stiffness model and the contact-bond model are employed to represent the interactions within aggregates. The linear contact-stiffness model is employed to represent the interactions between adjacent aggregates. Considering the closed packing cubic arrays of discrete elements (each with six neighbors) in the developed DE model, the micro-stiffness of aggregate elements is determined based on the following equations^[12]:

$$E = \frac{k_n}{2t}$$

$$k_s = \frac{k_n}{2(1+\nu)}$$

where E is the apparent Young's modulus; k_n is the input normal stiffness; k_s is the input shear stiffness; and t is the disk thickness. The aggregate modulus is fixed at 55.5 GPa^[5].

In this study, the main purpose is to simulate the permanent deformation of asphalt mixtures. Bond breakage

within the DE model is suppressed by using a very high bond strength value.

2.3 Time-temperature superposition principle

The DE viscoelastic model can better simulate the viscoelastic behavior of asphalt mixtures. However, it is very time-consuming to run the DE viscoelastic model if real loading time is involved^[11]. Therefore, in order to reduce the computation time, an approach based on the TTS principle is developed in this study. The underlying bases for the TTS principle is that the processes involved in molecular relaxation or rearrangements in the viscoelastic materials occur at accelerated rates at higher temperatures, and there is a direct equivalency between time and temperature for a viscoelastic material. Hence, the loading time can be reduced by conducting the measurement at elevated temperatures and then shifting the resultant data to lower temperatures. This time-temperature equivalency can be more clearly expressed by the following equations:

$$\varepsilon(T, t) = \varepsilon(T_r, t_r) \quad (9)$$

$$t = \alpha_T t_r \quad (10)$$

where $\varepsilon(T, t)$ is the creep strain at the real temperature and loading time; $\varepsilon(T_r, t_r)$ is the creep strain at the reference temperature and reduced loading time; T and t are the real temperature and loading time, respectively; T_r and t_r are the reference temperature and reduced loading time, respectively; and α_T is the shifting factor.

The creep strain in the viscoelastic Burger's model at real temperature can be expressed as

$$\varepsilon(T, t) = \sigma_0 \left[\frac{1}{E_1} + \frac{t}{\eta_1} + \frac{1}{E_2} (1 - e^{-(E_2/\eta_2)t}) \right] \quad (11)$$

If the real temperature increases up to the reference temperature, the viscoelastic properties will be changed. Assuming that E_1 , E_2 , η_{1r} and η_{2r} are the Burger's model parameters at the reference temperature, the creep strain at the reduced time can be expressed as

$$\varepsilon(T_r, t_r) = \sigma_0 \left[\frac{1}{E_1} + \frac{t_r}{\eta_{1r}} + \frac{1}{E_2} (1 - e^{-(E_2/\eta_{2r})t_r}) \right] \quad (12)$$

By solving Eqs. (9) to (12), the Burger's model parameters at the reference temperature are determined as follows:

$$\eta_{1r} = \frac{\eta_1}{\alpha_T} \quad (13)$$

$$\eta_{2r} = \frac{\eta_2}{\alpha_T} \quad (14)$$

As the Burger's model parameters at the reference temperature are used, the same creep strain is determined by the reference Burger's model parameters and the reduced

time. Therefore, the computation time is dependent on the reduced time instead of the real time. Since the reduced time is much smaller than the real time when the shifting factor is very large, the computation time is supposed to be reduced significantly. The trial calculation results show that a value less than 10^4 is considered as a reasonable shifting factor without affecting the final simulation results.

2.4 Virtual rutting test

According to the rutting test specifications^[13], the specimen is molded with a size of 300 mm \times 50 mm, and the wheel rolls on the specimen surface back and forth 42 times per minute for 1 h at 60 °C. The mass of the loading wheel is 78 kg, and the contact pressure is 0.7 MPa. The wheel rolling distance and the wheel width is 230 mm and 50 mm, respectively.

Since the loading mode of the 2D virtual rutting test is different from that of the laboratory rutting test, the cumulative loading time that the wheel covers on one point on the specimen surface is regarded as the total loading time in the 2D virtual rutting test. The contact length can be calculated from the following equation:

$$mg = pA = p(dl) \quad (15)$$

where m is the mass of the loading wheel; g is the acceleration of gravity; p is the contact pressure; d is the wheel width; l is the contact length between the wheel and the specimen.

$l = 21.84$ mm is calculated from Eq. (15). Therefore, the cumulative loading time of one point on the specimen surface is $3\,600 \times l/230 = 342$ s. When applying the shifting factor of 10^4 , the computation time is significantly reduced to 0.034 2 s. The virtual specimen is loaded by walls with the servo-control program to obtain a contact pressure of 0.7 MPa. The rutting formation process is shown in Fig. 5.

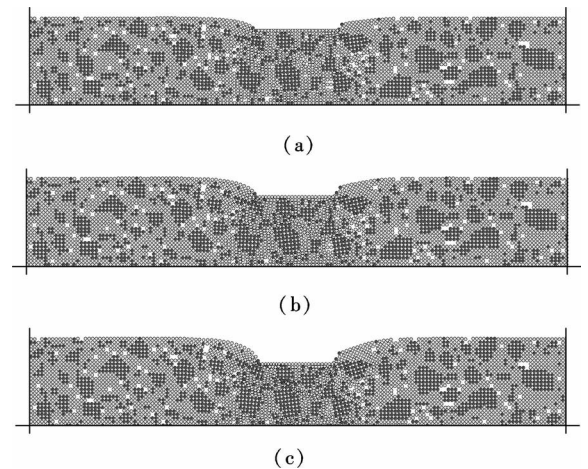


Fig. 5 Formation of rutting in virtual rutting test. (a) $t = 0.011\,4$ s; (b) $t = 0.022\,8$ s; (c) $t = 0.034\,2$ s

The displacement field at the end of the virtual test is shown in Fig. 6. It can be seen that the vertical displacement dominates in the loading area while the minor lateral displacement appears on both sides of the loading area. It is indicated that the deformation is induced mainly by compaction. The vertical deformation curve of the asphalt mixture is shown in Fig. 7.



Fig. 6 Displacement field at the end of virtual rutting test

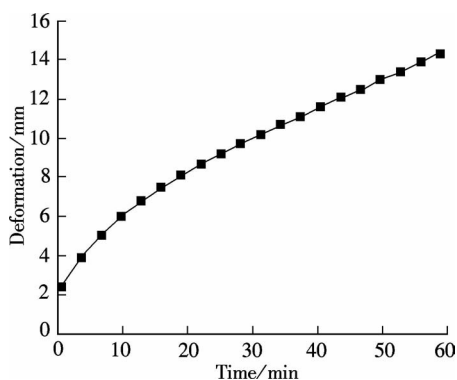


Fig. 7 Deformation curve in virtual rutting test

3 Verification of Virtual Rutting Test

In order to verify the virtual rutting test, laboratory rutting tests are conducted on a group of asphalt mixtures with the same gradations (see Tab. 3), and the comparison results are shown in Tab. 4. As shown in Tab. 4, the deformation and the dynamic stability in the virtual rutting test are slightly greater than those in the experiments.

The reason is that there are more aggregates in contact in the laboratory-compacted specimen, which results in stronger interlocks among aggregates. However, there are

Tab. 3 Aggregate gradations

Sieve size/mm	Percentage passing/%		
	Gradation 1 [#]	Gradation 2 [#]	Gradation 3 [#]
19.00		100	100
16.00	100	95	90
13.20	92	84	76
9.50	80	70	60
4.75	62	48	34
2.36	48	34	20

Tab. 4 Comparison between virtual rutting test and laboratory measurements

Gradation	Deformation/mm		Dynamic stability/ (times · mm ⁻¹)	
	Laboratory test	Virtual test	Laboratory test	Virtual test
1 [#]	13.4	15.3	882	808
2 [#]	12.2	14.4	970	859
3 [#]	11.2	12.6	1 274	984

fewer aggregate contacts in the 2D model. Therefore, the laboratory-compacted specimen has a higher resistance to load than the 2D model. In addition, since fine aggregates are integrated into the asphalt mastic, the resistance to the load of the 2D model will also be weakened. It is indicated that the virtual rutting test using the DEM can predict the permanent deformation performance of asphalt mixtures. For a more precise prediction, a three-dimensional (3D) DE model will be desired.

4 Conclusions

1) The virtual rutting test is developed including the development of the DE model of asphalt mixtures, the representation of different interactions within asphalt mixtures, the determination of the micromechanics model parameters and the way of loading.

2) The approach based on the TTS principle in the DE viscoelastic model can significantly reduce the computation time, which can greatly promote the application of the DE viscoelastic model of asphalt mixtures.

3) The deformation law of asphalt mixtures in the virtual rutting test is similar to the laboratory measurements, and the deformation and the dynamic stability of the virtual rutting test are slightly greater than those in the experiments. The 2D virtual rutting test can predict the permanent deformation performance of asphalt mixtures.

References

- [1] Hu X G. Review on asphalt mixture micromechanics analysis [J]. *Journal of Chang'an University: Natural Science Edition*, 2005, **25**(2): 6–9. (in Chinese)
- [2] Tan J Q. Study on coarse aggregate shape characteristics and virtual test of gradation [D]. Guangzhou: School of Civil Engineering and Transportation of South China University of Technology, 2006. (in Chinese)
- [3] Chang G K, Meegoda J N. Micromechanical simulation of hot mixture asphalt [J]. *Journal of Materials in Civil Engineering*, 1997, **123**(5): 495–503.
- [4] Buttlar W G, You Z P. Discrete element modeling of asphalt concrete: microfabric approach [J]. *Transportation Research Record*, 2001, **1757**: 111–118.
- [5] You Z P, Buttlar W G. Discrete element modeling to predict the modulus of asphalt concrete mixtures [J]. *Journal of Materials in Civil Engineering*, 2004, **16**(2): 140–146.
- [6] Collop A C, McDowell G R. Use of the distinct element method to model the deformation behavior of an idealized asphalt mixture [J]. *International Journal of Pavement Engineering*, 2004, **1**(5): 1–7.
- [7] Abbas A, Masad E, Papagiannakis T, et al. Micromechanical modeling of the viscoelastic behavior of asphalt mixtures using the discrete-element method [J]. *International Journal of Geomechanics*, 2007, **7**(2): 131–139.
- [8] Kim H, Wagoner W P, Buttlar W G. Simulation of fracture behavior in asphalt concrete using a heterogeneous cohesive zone discrete element model [J]. *Journal of Materials in Civil Engineering*, 2008, **20**(8): 552–563.

- [9] Saltykov S A. *Stereometric metallography* [M]. Moscow: State Publishing House for Metals and Sciences, 1958.
- [10] Dehoff R T, Rhines F N. *Quantitative microscopy* [M]. New York: McGraw Hill, 1968.
- [11] Liu Y, Dai Q L, You, Z P. Viscoelastic model for discrete element simulation of asphalt mixtures [J]. *Journal of Engineering Mechanics*, 2009, **135**(4): 324–333.
- [12] Thornton C. The conditions for failure of a face-centered cubic array of uniform rigid spheres [J]. *Geotechnique*, 1979, **29**(4): 441–459.
- [13] Ministry of Transport of the People's Republic of China. JTJ 052—2000 Standard test methods of bitumen and bituminous mixtures for highway engineering [S]. Beijing: China Communications Press, 2000. (in Chinese)

基于离散元法的沥青混合料虚拟车辙试验

张德育 黄晓明 高英

(东南大学交通学院, 南京 210096)

摘要:为了从沥青混合料不连续特征角度研究其永久变形行为,采用离散元方法进行了沥青混合料虚拟车辙试验.根据概率理论及蒙特卡洛方法,编写了考虑集料级配及不规则形状的沥青混合料二维数字试件生成程序.在生成的数字试件基础上进行了沥青混合料离散元虚拟车辙试验,并利用基于时温等效原理的计算方法以减少虚拟车辙试验的计算时间.最后将模拟结果与室内试验结果进行了比较.研究表明:基于时温等效原理的离散元黏弹性模型计算方法可以大大减少计算时间;虚拟车辙试验中沥青混合料变形情况与室内车辙试验相似,虚拟车辙试验的变形量及动稳定度略大于室内车辙试验;建立的沥青混合料二维虚拟车辙试验能够预测沥青混合料的永久变形性能.

关键词:沥青混合料;永久变形;离散元法;虚拟车辙试验

中图分类号:U414